Attractive Nanocolloid−Polymer Mixtures: Comparison of a Modified Perturbed Lennard-Jones Equation of State to Monte Carlo Simulation

Carlos A. Quant and J. Carson Meredith*

School of Chemical and Biomolecular Engineering, Georgia Institute of Technology, Atlanta, Georgia 30332-0100

Received August 31, 2004; Revised Manuscript Received October 22, 2004

ABSTRACT: The development of predictive equations of state for nanoparticle−surfactant or −polymer mixtures is of extreme importance in nanotechnology and fabrication of advanced materials. Of particular interest is modeling the transitional regime between entropy-controlled (depletion, repulsive interactions) vs enthalpy-controlled physics (adsorption, attractive interactions). In this paper, the perturbed Lennard-Jones chain (PLJC) equation of state (EOS)[1] for polymer−solvent mixtures is modified and extended to calculate the chemical potentials in nanoparticle−polymer mixtures. The EOS predictions are compared to Monte Carlo simulations that use the same LJ molecular model over a wide range of polymer concentrations approaching the semidilute regime, $0.15 < c_p/c_p^* < 0.8$. The original PLJC equation, with one adjustable parameter, predicts the nanoparticle chemical potential very well for the enthalpy-dominated *strong adsorption regime,* e.g., LJ energy parameters $\epsilon_{cp} > \epsilon_{pp}$, where ϵ_{cp} = colloid−polymer and ϵ_{pp} = polymer−polymer. However, for LJ parameters leading to weak polymer adsorption or depletion, $\epsilon_{cp} < \epsilon_{pp}$, the PLJC could not predict simulation results without further modification. We introduced a semiempirical term that corrects for the polymer−colloid excluded volume. The correction introduces one additional adjustable parameter, but this parameter remained essentially unchanged for all particle compositions, sizes, and ϵ_{cp} values studied. These results illustrate that a polymer equation of state, when corrected for the polymer−particle excluded volume, holds promise in modeling the effects of attractive polymeric modifiers on nanoparticle dispersions.

1. Introduction

Nanotechnology is an interdisciplinary area of research that has recently emerged as one of the most promising areas of scientific study because of its potential to revolutionize the synthesis and processing of materials. Nanoscale materials display exceptional physical and chemical characteristics that depend sensitively on dimensions and composition. Much research has been focused on discovering suitable ways to use self-assembly to fabricate and organize colloidal nanoparticles efficiently and reliably into practical materials. In many cases polymers and oligomers are used to stabilize nanoparticle suspensions or to direct self-assembly. Variations in the modifier chain length, adsorption, and chemistry can be used to control the stability of colloidal dispersions.[2] Recent examples include nanocolloid silica particles grafted with polystyrene−poly(benzyl acrylate) block copolymer chains,[3] self-assembled multidimensional structures of metal nanocrystals with the aid of alkanethiols,[4,5] and Pd nanoparticles synthesized by stabilization with poly(vinylpyrrolidone).[6] Experiments indicate profound differences in suspension structure when particle interactions are varied from repulsive to attractive. A vast literature treats the theory of purely repulsive nanoparticle−polymer mixtures,[7−17] and predictive models have been constructed for the phase behavior of these depletion systems.[12,13,15,18,19] Unfortunately, the theory and modeling of attractive polymer−nanoparticle mixtures has received far less attention, and little is known about the transition between strongly repulsive and strongly attractive regimes of nanoparticle−polymer interactions.

* To whom correspondence should be addressed: carson.meredith@che.gatech.edu.

Thermodynamic chemical potential models that can be used to predict the phase behavior of polymer−nanoparticle mixtures are as essential to nanotechnology as they have been in conventional chemical processing. The chemical potential, defined in a mathematically rigorous manner in classical and statistical thermodynamics, provides valuable information on the local environment of molecules or particles. A number of theoretical,[7,8,15,20−23] experimental,[24] and simulation[25,26] studies of polymer−nanocolloid systems (this list is by no means exhaustive) calculate chemical potentials or related properties. Most of these have focused on *hard-sphere repulsive systems*, where depletion physics is primarily responsible for phase behavior.[9,17−19] Recently, expanded ensemble Monte Carlo (EEMC)[27−29] simulations were adapted to calculate the *infinite dilution* chemical potential of nanoparticles[30] dispersed with freely adsorbing[31] attractive Lennard-Jones (LJ) polymers. These studies indicated that the nanoparticle chemical potential could be "switched" between excluded volume (entropy) controlled or adsorption (enthalpy) controlled physics by adjusting the LJ energy parameters.

Extensive research and effort have been centered on developing analytical equations of state (EOS) for attractive polymer solutions.[32−39] In this paper, we investigate the use of the perturbed Lennard-Jones chain (PLJC) EOS[1] as a foundation for a nanoparticle−polymer EOS. The PLJC is based on a first-order variational perturbation for attractive LJ chains[40,41] that uses a hard-sphere reference system[42] to represent repulsive interactions. For testing of the applicability of the PLJC to nanoparticle dispersions, EEMC simulations of LJ polymer−particle mixtures were performed over a wide range of polymer concentrations, approaching the semidilute crossover concentration. The simulations provide a well-defined system to which the model

10.1021/ma0482213 CCC: $30.25
Published on Web 12/13/2004

can be validated, since they both use the same LJ molecular interaction potential.

The remaining parts of this paper are organized as follows: In section 2, a brief description of the model system and EEMC simulation details is given. This section also includes the original PLJC equation[1] extended to polymer−nanocolloid mixtures and our modifications to account for asymmetric polymer and colloid LJ energy parameters. Section 3 presents and discusses the comparison between EEMC simulations and the PLJC EOS extended for nanocolloid−polymer mixtures, followed by the concluding remarks in section 4.

2. Theory and Simulation Methodology

2.1. Nanocolloidal Particle in the Presence of Freely Adsorbing Polymer Solution. The expanded ensemble Monte Carlo (EEMC) method[27,43] was applied to a system consisting of a single nanocolloidal particle in a dispersion of freely adsorbing fully flexible polymer chains in a continuum solvent. We calculated the particle and polymer chain chemical potentials and the polymer adsorption as a function of the chain length (n), colloid diameter (σ_c), and polymer segment density (ρ_p = number of segments/box volume), where volume is in units of the polymer segment diameter, σ_c^3. The chain lengths in the polymer solution were varied from sizes $n = 5$ to $n = 30$. The effects of polymer segment density with reference to the work by Marla and Meredith[31] were also investigated at higher polymer segment number densities where $\rho_p = 0.16$, 0.18, 0.20, 0.25, and 0.30. These polymer densities correspond to a range of c_p/c_p^* (polymer molar concentration:polymer semidilute crossover concentration ratio) of 0.15−0.78. This investigation studied the effects of varying the colloid particle diameter (σ_c) over $1\sigma_p \le \sigma_c \le 10\sigma_p$ on the colloidal particle chemical potential (μ_c). The system was held at a constant reduced temperature, $T^* = 3.0$, which has been shown to reproduce good solvent conditions for bulk solutions and to be above the theta T^* of 2.5 for this Lennard-Jones polymer model.[44]

The polymer chains are represented by using the self-avoiding random walk model in a good solvent. The chains are made up of freely jointed tangential Lennard-Jones spherical segments with bond length σ_p. The nanocolloid was modeled as an LJ sphere with diameter σ_c. The solvent molecules are not explicitly accounted for in the simulation, but one can vary the reduced temperature (T^*), therefore reducing the relative contribution of the attractive and repulsive interactions, to simulate the enthalpic effects of different types of solvents.

Two types of interactions were taken into account: nonbonded polymer segment−segment interactions and polymer segment−colloid interactions. To achieve efficiency in the calculation of energies and because the calculation of the nonbonded energies requires the greatest computational effort, the polymer segment−segment interactions were modeled using a truncated 6−12 Lennard-Jones potential where the force and energy are zero at $r_c \ge 2.5\sigma_p$ as described by Marla and Meredith.[31] The model of the LJ potential cutoff is shown in eq 1[31]

$$u(r_{ij}) = \begin{cases} 4\epsilon_{ij}\left[\left(\frac{\sigma_{ij}}{r_{ij}}\right)^{12} - \left(\frac{\sigma_{ij}}{r_{ij}}\right)^{6} - \left(\frac{\sigma_{ij}}{r_c}\right)^{12} + \left(\frac{\sigma_{ij}}{r_c}\right)^{6}\right] & r > r_c \\ 0 & r \le r_c \end{cases} \quad (1)$$

where r is the distance between interacting sites in the simulation, ϵ_{ij} is the energy interaction parameter, and $\sigma_{ij} = {}^1/_2(\sigma_i + \sigma_j)$ is the size parameter. For the polymer segment−colloid interactions the full LJ potential with no cutoff was used since no considerable reduction in computational effort would be gained from a cutoff potential. It should be noted that the 6−12 LJ potential is not an experimentally realistic model for the system at hand due to the fact that the this potential was derived for point−point interactions. For the colloid−polymer interaction, an integration of the LJ potential for each of the atoms that make up the colloid and each polymer segment would be a better approximation. It has been shown that such an integration would result in a potential proportional to $\sim\{(\sigma/r)^9 - (\sigma/r)^3\}$.[45,46] The LJ point model does, however, capture some of the essential physics of van der Waals dispersion interactions.[31]

2.2. Expanded Ensemble Monte Carlo Simulation Methodology. The EEMC method was employed to calculate the excess chemical potential of the colloidal particle and of the polymer chains. To ensure the system achieved thermal equilibrium, random translation and displacement of the colloid and chain segments was attempted and accepted according to the standard Metropolis Monte Carlo[47] criterion (colloid) or the continuum configurational bias (CCB)[23,48] criterion (polymer).

All simulations were performed using periodic boundary conditions in a cube with length $l = 40\sigma_p$ to avoid any self-interaction through the periodic boundaries.[31] The reduced variables used in the simulation were $T^* = Tk_B/\epsilon_{pp}$, $\rho_p^* = \rho_p\sigma_p^3$, and $\rho_p = Mn/V$, where T is the temperature, k_B is the Boltzmann constant, ϵ_{pp} is the polymer segment−segment interaction energy, M is the number of chains, and V is the volume of the simulation box. A general overview of the method will be described below; a more complete and detailed description can be found elsewhere.[27−30,49] The expanded ensemble method (EE) calculates chemical potentials by using additional ensemble variables[27,43,50] that are adjusted to define a smooth and reversible path for the measurement of the free energy between different states of the system.[28,29,49] In the case of the particle chemical potential, the additional expansion variable is the diameter of the colloidal particle. The EE method applied to the calculation of colloid particle chemical potential has been shown[31] to increase the efficiency at which the particle chemical potential is calculated and avoids the uncertainties and steric overlaps of other particle insertion methods such as the Widom[51] and inverse Widom.[52] The simulation calculates the incremental colloid particle chemical potential ($\beta\mu_{ci}^{ex}$) at each predetermined colloidal diameter increment by[31]

$$\beta\mu_c^{ex} = -\ln\left[\exp\left(\frac{-\Delta E_i}{k_B T}\right)\right] \quad (2)$$

where ΔE_i is the energy change in the system due to the increment in the colloidal diameter from σ_{ci-1} to σ_{ci}. Each increment or decrement is accepted or rejected using an acceptance criterion similar to Metropolis.[47] The sum of all incremental values, $\sum\beta\mu_{ci}^{ex}$, gives $\beta\mu_c^{ex}$ for the full sized colloidal nanoparticle (σ_c), where it is recognized that $\beta\mu_c^{ex}$ is the *configurational* particle chemical potential. The full (thermodynamic) potential, $\beta\mu_c$, is obtained by adding to this the ideal contribution

Table 1. Reduced Polymer Concentration (c_p/c_p^*) and Radius of Gyration (R_g) for Different Polymer Segment Densities and Chain Lengths Studied for the EEMC Simulations

	ρ_p	R_g	$c_p/c_p^* = {}^4/_3(\pi/n)\rho_p R_g^3$
$n = 5$	0.18	1.0017	0.1476
	0.20	1.0016	0.1684
	0.24	1.0011	0.2059
$n = 10$	0.16	1.5636	0.2598
	0.18	1.5618	0.2804
	0.20	1.5609	0.3186
	0.24	1.5592	0.3869
$n = 20$	0.18	2.3632	0.4862
	0.20	2.3621	0.5517
	0.24	2.3580	0.6697
$n = 30$	0.16	2.9810	0.6007
	0.18	2.9980	0.6621
	0.20	3.0188	0.7788

$\beta\mu_c^{id} = \ln(\rho_c)$, which goes to zero in the limit of infinite dilution. Since the method for calculating the particle and the chain chemical potential are similar, the reader is referred to recent publications by Escobedo and de Pablo[23,27,43,53] for the details of the calculation of the chemical potential for polymer chains using the EE method. As was mentioned earlier, the CCB algorithm is used to perform chain displacements by regrowing a predetermined part of the chain into a lower energy conformation while avoiding overlaps with neighboring chains segments and with the colloidal particle. A more rigorous treatment of the CCB method is shown in refs 48, 54, and 55. Absolute adsorption of chain segments per unit surface area of the colloidal particle was also calculated by integration of the segment density profile near the particle surface. A detailed description of this procedure is shown in ref 31.

To obtain statistically significant results for the variables studied (R_g, $\beta\mu_c^{ex}$, etc.), the simulations were averaged over 100−200 × 10^6 steps, where one step corresponds to one attempted move. As was shown in ref 31, 20% of the total moves attempted were colloid moves divided equally, that is, 10% Metropolis-type colloid displacement and 10% colloid EE moves. The remaining steps were chain moves divided equally between EE and CCB moves. Table 1 shows the polymer radius of gyration (R_g) and the reduced polymer concentration ($c_p/c_p^* = {}^4/_3(\pi/n)\rho_p R_g^3$) for all the system conditions studied in this investigation. Statistical analysis based on the inefficiency parameter[56] was performed on the simulation results and are presented in the Results and Discussion section.

2.3. PLJC Equation of State for Nanocolloid and Polymer Mixtures. Extensive research has centered on deriving analytical EOS for polymers and their solutions.[32−39] Recently, Lee et al.[1] derived a perturbation theory EOS for polymer−polymer and polymer−solvent liquid−liquid equilibria, known as the perturbed Lennard-Jones chain EOS. Since very few robust models and EOS for attractive nanocolloid−polymer systems exist and since the PLJC molecular model matches our simulation exactly, we used the PLJC as the foundation to propose a polymer−colloid EOS. This provides an unusual opportunity to compare EOS predictions to simulation results.

The PLJC's treatment of the polymer chain is similar to the EEMC simulation's treatment[31] where the chains are made up of freely jointed tangential LJ segments with bond length σ_p. The solvent molecules are treated as spherical LJ particles with size σ_s. The PLJC has three characteristic parameters equivalent to those used in the EEMC simulations: the chain length (n), the segmental interaction energy (ϵ_{ij}), and the segment size (σ) that are equivalent to the MC simulation parameters. Details of the derivation of the PLJC for polymer mixtures and polymer−solvent systems are shown elsewhere.[1,39−41,57] A summary of the method is described below. The PLJC is composed of two parts: one is a hard-sphere chain model used as a convenient reference system, and the other is a perturbation term derived from perturbation or variational theories. The excess Helmholtz energy A_{mixt} for the colloid−polymer mixture is[1]

$$\frac{A_{mixt}}{Nk_BT} = \frac{A_{mixt}^{HSC}}{Nk_BT} + \frac{A_{mixt}^{PERT}}{Nk_BT} \tag{3}$$

where N is the sum of the number of polymer segments and colloidal particles. The excess Helmholtz energy for the hard-sphere reference is defined as[41]

$$A_{mixt}^{HSC} = Nk_BT^*\left[\left(\frac{\zeta_2^3}{\zeta_0\zeta_3^2} - 1\right)\ln(1-\zeta_3) + \frac{3\zeta_1\zeta_2}{\zeta_0(1-\zeta_3)} + \frac{\zeta_2^3}{\zeta_0\zeta_3(1-\zeta_3)^2}\right] + \phi_{cc}\left(1 - \frac{1}{n_c}\right)\left[\ln(1-\zeta_3) - \frac{3\zeta_1 d_{cc}}{2(1-\zeta_3)}\right] + \phi_{pp}\left(1 - \frac{1}{n_p}\right)\left[\ln(1-\zeta_3) - \frac{3\zeta_1 d_{pp}}{2(1-\zeta_3)}\right] \tag{4}$$

where

$$\zeta_j = \frac{\pi}{6}\sum_i n_i\rho d_{ii}^{\,j} \tag{5}$$

$$\phi_{ii} = \frac{x_i n_i}{\sum_j x_j n_j} \tag{6}$$

$$\left(\frac{2^{1/6}}{a_{ii}} - 1\right)^3 = \left(\frac{0.005397n_i + 0.006354}{9.44 + n_i}\right)T^* + \left(\frac{0.01222n_i + 0.005102}{9.947 + n_i}\right) \tag{7}$$

n_i is either the number of segments in a polymer chain (n_p) or colloid (n_c). $n_c = 1$ since the number of segments that make up a colloid is one. x_i is the fraction of chain segments or colloid particles in the system, ρ is the total number density, and d_{ii} ($d_{ii} = a_{ii}\sigma_{ii}$) is the optimal dimensionless diameter of a hard-sphere segment obtained from numerical minimization of the free energy of the system which is then fitted to the expression shown in eq 7.[39]

From a variational first-order perturbation theory, von Solms et al.[41] derived the attractive (perturbation) term as shown in eq 8, which has been modified with minor changes to reflect the colloid−polymer system at hand.

$$A_{\text{mixt}}^{\text{PERT}} = 2\pi\rho N\epsilon_{cc}\left\{\phi_c^2 n_c^2\left(\frac{\sigma_{cc}}{a_{cc}}\right)^3\left[I_{A_{cc}} + I_{B_{cc}}\left(\frac{1}{a_{cc}^6} - 1\right)\right]\right\} + \phi_c\phi_p n_c n_p v_p \frac{\epsilon_{cp}}{\epsilon_{cc}}\left(\frac{\sigma_{cp}}{a_{cp}}\right)^3\left[I_{A_{cp}} + I_{B_{cp}}\left(\frac{1}{a_{cp}^6} - 1\right)\right] + \phi_p^2 n_p^2 v_p^2 \frac{\epsilon_{pp}}{\epsilon_{cc}}\left(\frac{\sigma_{pp}}{a_{pp}}\right)^3\left[I_{A_{pp}} + I_{B_{pp}}\left(\frac{1}{a_{pp}^6} - 1\right)\right] \quad (8)$$

where ν_p is an empirical parameter that will be discussed later and $I_{A_{ii}}$ and $I_{B_{ii}}$ are perturbation integrals which have been fitted to analytical expressions as shown in eqs 9 and 10.[1,39]

$$I_{A_{ii}} = [(-0.22169n_i - 1.0755) - (2.2618n_i - 1.0385)\zeta_3 + (1.47n_i - 0.55411)\zeta_3^2]/(0.4571 + n_i) \quad (9)$$

$$I_{B_{ii}} = \left(0.03171 + \frac{0.4213}{n_i}\right) + \left(0.66264 + \frac{0.0987}{n_i}\right)\zeta_3 + 1.7866\zeta_3^2 \quad (10)$$

The average between the polymer−polymer and colloid−colloid parameters (such that $M_{ij} = {}^1/_2\{M_{ij} + M_{ij}\}$) was used as the mixing rule for σ_{ij}, d_{ij}, IA_{ij}, and IB_{ij}. For the ϵ_{ij} and a_{ij} the following mixing rules were used: $\epsilon_{cp} = \sqrt{\epsilon_{cc}\epsilon_{pp}}$ and $a_{cp} = (a_{pp}\sigma_{pp} + a_{cc}\sigma_{cc})/(\sigma_{pp} + \sigma_{cc})$.

The governing equation that relates the Helmholtz free energy to the chemical potential is eq 11. Because of the cumbersome nature of deriving an analytical solution to eq 11, a numerical method approach was chosen instead. The forward finite divided difference (FFDD) numerical differentiation technique was used to evaluate eq 11. Since the infinite particle dilution $\beta\mu_c$ is to be calculated, the central finite divided difference (CFDD) or the backward finite divided difference (BFDD) could not be employed since they require data points outside the available range. Equation 12 shows the FFDD formula used, where h is the step size.

$$\beta\mu_c = \left.\frac{\partial A_{\text{mixed}}}{\partial n_c}\right|_{n_p,T,V} \quad (11)$$

$$f'(x_i) = \frac{-f(x_{i+2}) + 4f(x_{i+1}) - 3f(x_i)}{2h} \quad (12)$$

The empirical parameter ν_p (from eq 8), introduced by Hino et al.[58] for a perturbed hard-sphere-chain EOS and further extended by Lee et al.[1] for the PLJC, has been used successfully to predict phase behavior of various polymeric solutions. This empirical term arises from the fact that the perturbation term overpredicts the attractive interactions between polymer chains. Hence, without this modification the PLJC incorrectly predicts phase separation under conditions where phases should be stable.[1] Because of the similarity between models (colloid−polymer system and solvent−polymer system), an analogous empirical parameter can be used in the EOS for the colloid−polymer system. The regression procedure described by Lee et al.[1] was adopted in this study to use the PLJC to model a nanocolloid and polymer surfactant mixture by adjusting the empirical parameter ν_p. The objective function of the regression was chosen to be the sum of squared error (SSE) between the predicted PLJC particle chemical potentials ($\beta\mu_{\text{PLJC}}$) and the EEMC simulation ($\beta\mu_{\text{MC}}$) and is shown in eq 13:

$$\text{SSE} = \sum_{i=1}^{d}\left(\frac{\beta\mu_{\text{PLJC}} - \beta\mu_{\text{MC}}}{\beta\mu_{\text{MC}}}\right)^2 \quad (13)$$

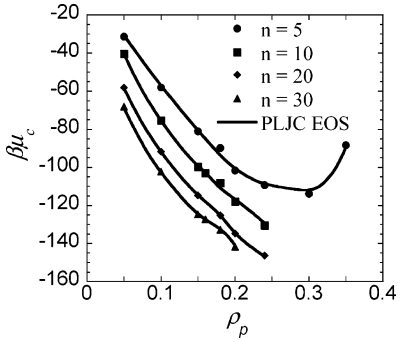

Figure 1. Infinitely dilute reduced particle chemical potential ($\beta\mu_c$) vs polymer segment density (ρ_p) at different chain lengths (n) for $\sigma_c = 10$. The solid markers (■) represent different values of simulation data, and the solid lines (—) represent the PLJC EOS.

3. Results and Discussion

3.1. Nanocolloid in Freely Adsorbing Polymer Solutions EEMC Simulation Results. 3.1.1. Effects of Polymer Density on Chemical Potential and Polymer Adsorption. Figure 1 shows a plot of particle chemical potential ($\beta\mu_c$) vs polymer density (ρ_p) for different chain lengths at a constant particle size $\sigma_c = 10$ and constant colloid−polymer interaction energy $\epsilon_{cp} = \epsilon_{pp} = 1$. It is noted that the confidence intervals have been omitted unless the error bars were larger than the markers representing simulation results. $\beta\mu_c$ decreases with increasing ρ_p and seems to be reaching a minimum value near a polymer density of $\rho_p \approx 0.30$. Computational restrictions have impeded the calculation of $\beta\mu_c$ at $\rho_p > 0.20$ and $n > 5$, and hence the minimum in $\beta\mu_c$ is only observed for $n = 5$. The observed trends are as expected since increasing the polymer density increases chain adsorption and lowers the particle chemical potential due to the polymer−colloid attractions. However, there is an increase in the excluded volume when polymer density increases, thereby increasing the difficulty of particle insertion. The μ_c trends are determined by competition between these two factors as ρ_p increases, resulting in a minimum value: entropy decreases due to increased excluded volume (more positive μ_c) and enthalpy decreases due to polymer adsorption (more negative μ_c). We note that a minimum in $\beta\mu_c$ with respect to ρ_p is a necessary, although not sufficient, condition for phase instability. The minimum would be followed by a maximum if phase instability were occurring. This may explain the difficulty in achieving equilibration of the simulations in the vicinity of the $\beta\mu_c$ minimum.

The effects of adsorption can be further appreciated with Figure 2, which shows a plot of absolute adsorption of polymer segments per unit surface area of the particle (Γ_s) vs polymer density (ρ_p) at $\sigma_c = 10$. Initially, as the polymer concentration increases, Γ_s increases because more chains are available to adsorb.

3.1.2. Effects of Particle Diameter on $\beta\mu_c$ and Adsorbed Amount. Figure 3 shows a plot of $\beta\mu_c$ vs diameter of the colloidal particle (σ_c) at $n = 10$ and ϵ_{cp}

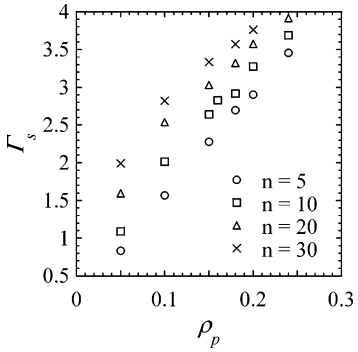

Figure 2. Absolute adsorption per surface area of the particle (Γ_s) vs polymer segment density (ρ_p) at different chain lengths (n) for $\sigma_c = 10$. The markers represent different values of simulation data.

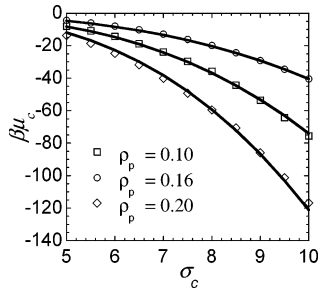

Figure 3. Infinite dilute chemical potential $\beta\mu_c$ vs colloid diameter (σ_c) at three different polymer segment densities (ρ_p) for $n = 10$. The markers represent EEMC simulation data at polymer segment densities of 0.10, 0.16, and 0.20; the solid line (—) represents the PLJC equation of state extended to nanocolloid−polymer mixtures.

$= \epsilon_{pp}$ for different values of polymer segment density (ρ_p). $\beta\mu_c$ decreases for all values of σ_c at high polymer densities. These results follow the same pattern as previously reported[31] for dilute polymer concentrations due to the dependence of the LJ potential on σ_c. Increasing σ_c increases the range of the LJ potential energy,[31] resulting in a larger number of polymers interacting attractively with the colloidal particle, which in turn decreases the chemical potential. Figure 4 illustrates the effects of colloid diameter (σ_c) on excess amount adsorbed (Γ^{ex}) (bottom) and the excess adsorption per unit surface area (Γ_s^{ex}) (top) for different polymer densities. Polymer excess adsorption (Γ^{ex}) increases with σ_c in two distinct ways: (1) in the region $0 < \sigma_c \leq 5$, Γ^{ex} increases slowly with σ_c and (2) for $\sigma_c > 5$, Γ^{ex} increases more rapidly. At lower particle diameters, the increase in the excess amount adsorbed is mostly due to the increase in the range of the LJ potential energy as previously mentioned. As the particle diameter enters the region where $\sigma_c > 5$, another factor in addition to the increase in the LJ potential energy becomes increasingly important: surface area of the particle. This is evidenced by the Γ_s^{ex} vs σ_c plot (Figure 4, top) where the amount adsorbed per surface area of the particle (Γ_s^{ex}) is greater at $\sigma_c < 5$ leveling out at $\sigma_c > 5$, suggesting that the observed adsorption regimes shown in Figure 4 (bottom) are most likely caused by the greater surface area that allows for more adsorption, resulting in the steeper curve at larger particle sizes. This suggests that, in the regime where the colloid is small relative to the polymer ($\sigma_c < 5$), Γ^{ex} is weakly dependent on ρ_p because there is less surface area for packing of adsorbed chains as compared to $\sigma_c > 5$.

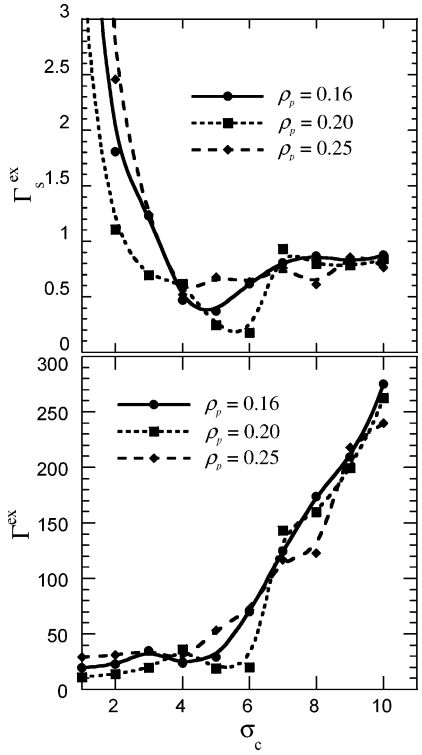

Figure 4. Excess amount adsorbed per unit surface (Γ_s^{ex}) and excess amount adsorbed (Γ^{ex}) vs colloid diameter (σ_c) at different polymer segment densities (ρ_p) for $n = 10$. The markers represent different values of simulation data. The lines are a visual aid.

3.2. PLJC EOS vs EEMC Simulation Results. Effect of the Parameter v_p. The PLJC EOS adapted for nanocolloid−polymer mixtures is compared to EEMC simulation results at various polymer concentrations (ρ_p), chain lengths (n), and colloid diameter (σ_c) in Figures 1 and 3. The PLJC EOS was able to model the behavior of colloid−polymer mixtures successfully for all cases where $\epsilon_{cp} = \epsilon_{pp}$ and for $\epsilon_{cp} = 1.5\epsilon_{pp}$ (not shown). As in the bulk PLJC for polymer solutions, it was necessary to include the empirical parameter ν_p. In the original PLJC the parameter ν_p ($0 < \nu_p \leq 1$) was used to correct the overestimated intersegmental attractive interaction between polymers.[1,38] A larger correction corresponds to smaller ν_p values. The variational perturbation neglects intrachain correlations, which become especially important at low ρ_p and low n, where mean-field estimations also fail. So, one expects that in bulk systems the correction will be greater, and hence ν_p smaller, as ρ_p and n decrease. In fact, Chiew et al.[1] and Prausnitz et al.[38] showed that $\nu_p \sim \rho_p$ and $\nu_p \sim n$ for bulk polymer solutions.

Our results for the PLJC applied to nanoparticle−polymer mixtures in Figure 5 show $\nu_p \sim 1/\rho_p$ and $\nu_p \sim 1/n$, which is *opposite* the trends for bulk polymer solutions. The value of ν_p decreases strongly with n^{-y} ($0.8 < y < 1.1$) but is only weakly dependent on ρ_p. In fact, not only is the dependence of ν_p on n opposite to bulk solutions, but for nanoparticles the ν_p magnitude ($0 < \nu_p \leq 0.2$) is much less than for polymer solutions ($0 < \nu_p \leq 1$). Consider that the primary differences between our system and bulk solutions are (1) chain adsorption on particles and (2) neglect of explicit solvent molecules. As polymer adsorption increases with chain length and polymer concentration, a densely packed layer develops close to the particle surface. The dense

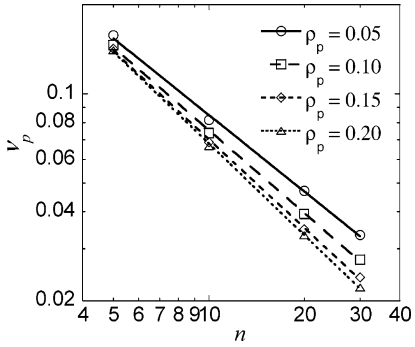

Figure 5. Log−log plot of the empirical parameter ν_p vs chain length (n) at different polymer segment densities (ρ_p). The markers represent the ν_p calculated by using the regression procedure outlined previously. The lines are power-law regressions.

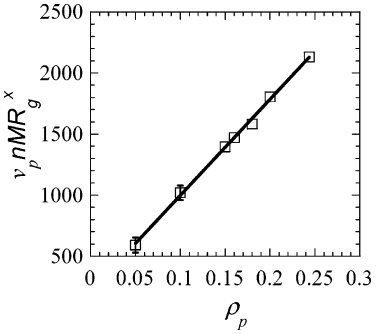

Figure 6. Average ($\nu_p R_g^x mn$) vs polymer segment densities (ρ_p) using data for all chain lengths (n). The markers represent averages calculated by using the regression procedure mentioned in section 3.2, where $x = 5/3$. The error bars represent 95% confidence intervals. Error bars that were smaller than the markers representing the data have been omitted.

adsorbed layers allow very strong attractions (polymer−polymer and polymer−colloid) not present in a bulk system, leading to enthalpy-dominated physical behavior. The absence of explicit solvent can also cause an overestimation of polymer−polymer interactions, as solvent would normally "screen" polymer−polymer interactions. Regression analysis on Figure 5 shows that the ν_p parameter for different n values can be collapsed to one master plot (Figure 6) by plotting $\nu_p MnR_g^x$ vs ρ_p, where R_g is the polymer radius of gyration from EEMC simulations and $x = 5/3$ is the exponent from least-squares regression. No quantitative molecular significance for the value of x could be drawn, but the discussion above indicates the qualitative molecular significance. Perhaps the qualitative dependence could be used to motivate predictions of ν_p for other conditions such as larger chain lengths and polymer densities.

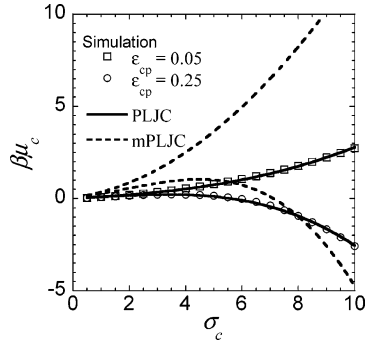

Figure 7. Infinite dilution colloid chemical potential ($\beta\mu_c$) vs colloid diameter (σ_c) at different interaction energies (ϵ_{cp}) for $n = 10$. The markers represent EEMC simulation data at ϵ_{cp} of 0.05 and 0.25, where the square markers (□) represent $\epsilon_{cp} = 0.05$ and the circular markers (○) represent $\epsilon_{cp} = 0.25$. The solid lines (—) represent the mPLJC equation of state with the inclusion of the correction term in eq 14, and the dotted lines represent the PLJC without the correction (···) for $\epsilon_{cp} = 0.05$ and (- - -) for $\epsilon_{cp} = 0.25$.

3.3. Correction for Adsorption Effects. Figure 7 shows that the PLJC EOS is unable to predict the behavior of weakly adsorbing polymer−nanoparticle mixtures when $\epsilon_{cp} < \epsilon_{pp}$. In this situation, the relative importance of polymer−colloid excluded volume (entropy) increases as compared to polymer−colloid attraction (enthalpy). The simulations indicate polymer desorption (relative to the $\epsilon_{cp} \geq \epsilon_{pp}$ case) and eventually depletion from the colloid surface as ϵ_{cp} is lowered further. Depletion is driven by the gain in polymer conformations away from the nanoparticle surface. Since the hard-sphere reference state of the PLJC was not developed to account for polymer−particle excluded volume (only polymer−solvent), the chemical potential is overpredicted when applied to the polymer−particle system under weak adsorption conditions. The PLJC model does not add the volume gained back when polymer desorbs. Although a correction for this effect might be obtained from analytical theories, for initial purposes we propose a simple semiempirical correction. The volume that the nanoparticle and polymer segments exclude from one another is approximately proportional to $(\sigma_c^2\sigma_p + \sigma_p^2\sigma_c)$. We propose a modification term, μ_{cp}, to be added to the colloid chemical potential in order to account for these effects.

$$\beta\mu_{cp} = C(\epsilon_{pp} - \epsilon_{cp})(\sigma_c^2\sigma_p + \sigma_p^2\sigma_c) \qquad (14)$$

Equation 14 is a simple semiempirical correction that "turns on" linearly as ϵ_{cp} becomes different from ϵ_{pp}. The constant C is determined via least-squares regression

Table 2. Corrected Chemical Potential ($\beta\mu$), Adsorption Correction ($\beta\mu_{cp}$), and the Constant C for Different Values of ϵ_{cp} and σ_c Studied for $\epsilon_{pp} = 1$

	$\epsilon_{cp} = 0.5$ $C = 0.1078$		$\epsilon_{cp} = 0.25$ $C = 0.1083$		$\epsilon_{cp} = 0.05$ $C = 0.1080$		$\epsilon_{cp} = 0.005$ $C = 0.1081$	
σ_c	$\beta\mu$	$\beta\mu_{cp}$	$\beta\mu$	$\beta\mu_{cp}$	$\beta\mu$	$\beta\mu_{cp}$	$\beta\mu$	$\beta\mu_{cp}$
1	0.079	0.108	0.087	0.162	0.097	0.205	0.108	0.215
2	0.104	0.324	0.169	0.486	0.205	0.616	0.211	0.645
3	−0.010	0.648	0.218	0.972	0.344	1.231	0.341	1.290
4	−0.343	1.080	0.210	1.620	0.519	2.052	0.506	2.149
5	−0.977	1.620	0.116	2.430	0.740	3.078	0.715	3.224
6	−1.993	2.268	−0.088	3.402	1.014	4.309	0.974	4.513
7	−3.473	3.024	−0.430	4.536	1.347	5.746	1.291	6.018
8	−5.497	3.888	−0.936	5.832	1.749	7.387	1.675	7.737
9	−8.148	4.860	−1.632	7.290	2.225	9.234	2.133	9.671
10	−1.508	5.940	−2.547	8.910	2.784	11.286	2.672	11.821

to obtain a fit to the experimental data, as indicated in Figure 7, resulting in values close to 0.108 in all cases explored. The modified PLJC, mPLJC, is obtained by adding $\beta\mu_{cp}$ to the $\beta\mu$ obtained in eq 11. Table 2 shows these values for all ϵ_{cp} and σ_c explored here. Figure 7 (solid lines) shows that the mPLJC correction allows nearly perfect agreement between theory and simulation. Since the C parameter is independent of composition and interaction parameters and chain lengths studied, the correction effectively adds no additional fitted parameters. The mPLJC requires only one truly adjustable parameter, v_p, which was also necessary for bulk solutions.

4. Conclusions

The EEMC method was extended to semidilute polymer concentrations for a nanocolloid in a freely adsorbing polymer solution. Simulation results were used to validate the predictions of the PLJC equation of state extended to model these polymer−nanocolloid dispersions. We identified two general regimes of physical effects of polymeric modifiers on nanoparticle thermodynamics. When $\epsilon_{cp} \geq \epsilon_{pp}$, the enthalpic regime, μ_c decreases with increasing ρ_p, approaching a minimum, while Γ increases. The minimum μ_c occurs because of competition between the enthalpic (attractive) and entropic (repulsive) effects of polymer adsorption. The PLJC EOS showed very good agreement with EEMC simulation results in this energetically controlled regime. The empirical parameter ν_p, introduced by others to correct the overly attractive perturbation (even in bulk polymer−solvent mixtures), was necessary to obtain agreement between theory and simulation in the polymer−nanoparticle case also. Furthermore, the collapse of ν_p values into one master plot as a function of n and ρ_p shows that ν_p can be predicted for other cases without having to regress additional simulation data.

The PLJC EOS did not predict accurately the simulation data for weak adsorption or depletion cases, e.g., $\epsilon_{cp} < \epsilon_{pp}$, a regime strongly influenced by entropy. This shortcoming is most likely due to the μ_c dependence on polymer−colloid excluded volume when the strength of attraction is diminished. We proposed a semiempirical modification term that corrects for polymer−colloid excluded volume. This modified "mPLJC" was able to predict the simulations very well for all cases, with an additional adjustable parameter whose value did not deviate significantly from ≈0.1 for all cases investigated.

References and Notes

(1) Chiew, Y.; Lee, Y.; Rangaiah, G. *Fluid Phase Equilib.* **2001**, *189*, 135−150.
(2) Cosgrove, T.; Fleer, G. J.; Cohen Stuart, M. A.; Scheutjen, J. M. H. M.; Vincent, B. *Polymer at Interfaces*, 2nd ed.; Chapman and Hall: London, 1993.
(3) Kowalewski, T.; McCullough, R. D.; Matyjaszewski, K. *Eur. Phys. J. E* **2003**, *10*, 5−16.
(4) Kulkarni, G. U.; Thomas, P. J.; Rao, C. N. R. *Pure Appl. Chem.* **2002**, *74*, 1581−1591.
(5) Murray, C. B.; Kagan, C. R.; Bawendi, M. G. *Science* **1995**, *270*, 1335−1338.
(6) Choo, H. P.; Liew, K. Y.; Liu, H. *J. Mater. Chem.* **2002**, *12*, 934−937.
(7) Fuchs, M.; Schweizer, K. S. *Phys. Rev. E* **2001**, *64*, 021514.
(8) Fuchs, M.; Schweizer, K. S. *J. Phys.: Condens. Matter* **2002**, *14*, R239−R269.
(9) Lekkerkerker, H. N. W.; Poon, W. C. K.; Pusey, P. N.; Stroobants, A.; Warren, P. B. *Europhys. Lett.* **1992**, *20*, 559−564.
(10) Roth, R.; Evans, R. *Europhys. Lett.* **2001**, *53*, 271−277.
(11) Piech, M.; Weronski, P.; Wu, X.; Walz, J. Y. *J. Colloid Interface Sci.* **2002**, *247*, 327−341.
(12) Maassen, R.; Eisenriegler, E.; Bringer, A. *J. Chem. Phys.* **2001**, *115*, 5292−5309.
(13) Louis, A. A.; Bolhuis, P. G.; Meijer, E. J.; Hansen, J. P. *J. Chem. Phys.* **2002**, *117*, 1893−1907.
(14) Gast, A. P.; Russel, W. B.; Hall, C. K. *J. Colloid Interface Sci.* **1983**, *96*, 251.
(15) Fuchs, M.; Schweizer, K. S. *Europhys. Lett.* **2000**, *51*, 621−627.
(16) Fleer, G. J.; Skvortsov, A. M.; Tuinier, R. *Macromolecules* **2003**, *36*, 7857−7872.
(17) Rotenberg, B.; Dzubiella, J.; Hansen, J.-P.; Louis, A. A. *Mol. Phys.* **2004**, *102*, 1−11.
(18) Ramakrishnan, S.; Fuchs, M.; Schweizer, K. S.; Zukoski, C. F. *Langmuir* **2002**, *18*, 1082−1090.
(19) Ramakrishnan, S.; Fuchs, M.; Schweizer, K. S.; Zukoski, C. F. *J. Chem. Phys.* **2002**, *116*, 2201.
(20) Aubouy, M.; Raphael, E. *Macromolecules* **1998**, *31*, 4357−4363.
(21) Sear, R. P.; Frenkel, D. *Phys. Rev. E* **1997**, *55*, 1677−1681.
(22) Nowicki, W. *Macromolecules* **2002**, *35*, 1424−1436.
(23) Escobedo, F. A.; de Pablo, J. J. *J. Chem. Phys.* **1995**, *102*, 2636−2652.
(24) Quant, C. A.; Meredith, J. C. Manuscript in preparation.
(25) Meijer, E. J.; Frenkel, D. *J. Chem. Phys.* **1994**, *100*, 6873.
(26) Meijer, E. J.; Frenkel, D. *Physica A* **1995**, *213*, 130−137.
(27) Escobedo, F.; de Pablo, J. J. *J. Chem. Phys.* **1995**, *103*, 2703−2710.
(28) Lyubartsev, A. P.; Martsinovski, A. A.; Shevkunov, S. V.; Vorontsov-Velyaminov, P. N. *J. Chem. Phys.* **1992**, *96*, 1776−1783.
(29) Wilding, N. B.; Muller, M. *J. Chem. Phys.* **1994**, *101*, 4324.
(30) Marla, K. T.; Meredith, J. C. *J. Chem. Phys.* **2002**, *117*, 5443−5451.
(31) Marla, K. T.; Meredith, J. C. *Langmuir* **2004**, *20*, 1501−1510.
(32) Radosz, M.; Huang, S. *Ind. Eng. Chem. Res.* **1990**, *29*, 2284−2294.
(33) Radosz, M.; Huang, S. *Ind. Eng. Chem. Res.* **1991**, *30*, 1994−2005.
(34) Shen, S.; Lu, B. *Fluid Phase Equilib.* **1993**, *84*, 9−22.
(35) Song, Y.; Lambert, S.; Prausnitz, J. M. *Ind. Eng. Chem. Res.* **1994**, *33*, 1047−1057.
(36) Song, Y.; Lambert, S.; Prausnitz, J. M. *Macromolecules* **1995**, *28*, 4866−4876.
(37) Tochigi, K.; Kurita, S.; Matsumoto, T. *Fluid Phase Equilib.* **1999**, *158*, 313−320.
(38) Prausnitz, J. M.; Hino, T.; Song, Y. *J. Polym. Sci., Part B: Polym. Phys.* **1996**, *34*, 1977−1985.
(39) Chiew, Y.; Chang, D.; Lai, J.; Wu, G. *Ind. Eng. Chem. Res.* **1999**, *38*, 4951−4958.
(40) O'Lenick, R.; Chiew, Y. *Mol. Phys.* **1995**, *85*, 257−269.
(41) von Solms, N.; Chiew, Y.; O'Lenick, R. *Mol. Phys.* **1999**, *96*, 15−29.
(42) Chiew, Y. *Mol. Phys.* **1990**, *70*, 129−143.
(43) Escobedo, F.; de Pablo, J. J. *J. Chem. Phys.* **1996**, *105*, 4391−4394.
(44) Lu, Y.; Tang, Y.; Sellinger, A.; Lu, M.; Huang, J.; Fan, H.; Haddad, R.; Lopez, G.; Burns, A.; Sasaki, D. Y.; Shelnutt, J.; Brinker, C. J. *Nature (London)* **2001**, *410*.
(45) Israelachvili, J. N. *Intermolecular & Surface Forces*, 2nd ed.; Academic Press: San Diego, 1991.
(46) Henderson, D.; Duh, D.-M.; Chu, X.; Wasan, D. *J. Colloid Interface Sci.* **1997**, *185*, 265−268.
(47) Metropolis, N.; Rosenbluth, A. W.; Rosenbluth, M. N.; Teller, A. H.; Teller, E. *J. Chem. Phys.* **1953**, *21*, 1087−1092.
(48) de Pablo, J. J.; Laso, M.; Suter, U. W.; Cochran, H. D. *Fluid Phase Equilib.* **1993**, *83*, 323−331.
(49) Kumar, K. S.; Szleifer, I.; Panagiotopoulos, A. Z. *Phys. Rev. Lett.* **1991**, *66*, 2935−2938.
(50) Escobedo, F.; de Pablo, J. J. *Mol. Phys.* **1996**, *89*, 1733−1754.
(51) Widom, B. *J. Chem. Phys.* **1963**, *39*, 2808−2812.
(52) Shing, K. S.; Gubbins, K. E. *Mol. Phys.* **1981**, *43*, 717- -721.
(53) Escobedo, F. A.; de Pablo, J. J. *Macromol. Theory Simul.* **1995**, *4*, 691−707.
(54) Siepmann, J. I. *Mol. Phys.* **1990**, *70*, 1145−1158.
(55) Mooij, G. C. A. M.; Frenkel, D. *Mol. Phys.* **1991**, *74*, 41−47.
(56) Allen, M. P.; Tildesley, D. J. *Computer Simulation of Liquids*, 1st ed.; Oxford University Press: Clarendon, Oxford, 1987.
(57) Chiew, Y.; O'Lenick, R. *Mol. Phys.* **1999**, *97*, 997−1008.
(58) Hino, T.; Song, Y.; Prausnitz, J. M. *J. Polym. Sci., Part B: Polym. Phys.* **1996**, *34*, 1961−1976.

MA0482213